Why Single-Beam Optical Tweezers Trap Gold Nanowires in Three Dimensions

Zijie Yan,[†] Matthew Pelton,[‡,⊥] Leonid Vigderman,[§] Eugene R. Zubarev,[§] and Norbert F. Scherer[†,*]

[†]The James Franck Institute and Department of Chemistry, The University of Chicago, 929 East 57th Street, Chicago, Illinois 60637, United States, [‡]Center for Nanoscale Materials, Argonne National Laboratory, 9700 South Cass Avenue, Argonne, Illinois 60439, United States, and [§]Department of Chemistry, Rice University, 6100 Main Street, Houston, Texas 77005, United States. [⊥]Present address: Department of Physics, University of Maryland, Baltimore County, 1000 Hilltop Circle, Baltimore, MD 21250.

ABSTRACT Understanding whether noble-metal nanostructures can be trapped optically and under what conditions will enable a range of applications that exploit their plasmonic properties. However, there are several nontrivial issues that first need to be resolved. A major one is that metal particles experience strong radiation pressure in optical beams, while stable optical trapping requires an attractive force greater than this radiation pressure. Therefore, it has generally been considered impossible to obtain sufficiently strong gradient forces using single-beam optical tweezers to trap relatively large metal nanostructures in three dimensions. Here we demonstrate that a single, tightly focused laser beam with a wavelength of 800 nm can achieve three-dimensional optical trapping of individual gold (Au) nanowires with lengths over 2 μm. Nanowires can be trapped by the beam at one of their ends, in which case they undergo significant angular fluctuations due to Brownian motion of the untrapped end. They can also be trapped close to their midpoints, in which case they are oriented approximately perpendicular to the light polarization direction. The behavior is markedly different from that of Ag nanowires with similar length and diameter, which cannot be trapped in three dimensions by a single focused Gaussian beam. Our results, including electrodynamics simulations that help to explain our experimental findings, suggest that the conventional wisdom, which holds that larger metal particles cannot be trapped, needs to be replaced with an understanding based on the details of plasmon resonances in the particles.

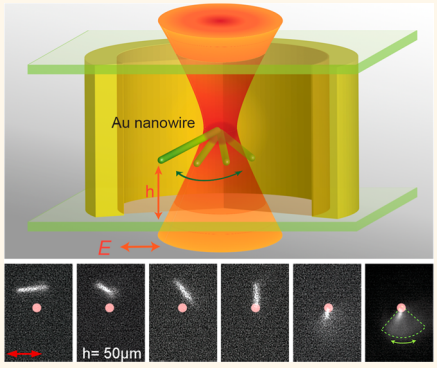

KEYWORDS: optical tweezers · Au nanowires · optical manipulation · plasmonics · nanophotonics

The unique size and morphology dependent optical properties of chemically synthesized noble metal nanostructures have attracted great interest.[1−3] These properties are largely determined by plasmon resonances, that is, the electromagnetic field-induced collective oscillations of their conduction electrons. Optical trapping of plasmonic nanostructures not only provides insight into fundamental light-matter interactions at the nanometer scale,[4−7] but also offers the possibility to manipulate and utilize individual nano-objects in sensing, biological, and medical applications.[3,8,9] Conventional optical tweezers, *i.e.*, single, tightly focused laser beams, have been successfully employed for three-dimensional (3D) trapping of silver (Ag) and Au nanoparticles,[10−12] as well as Au bipyramids and nanorods with aspect ratios up to 5.6.[13−15]

This approach, however, is problematic when the metal nanoparticles are further elongated into the nanowire regime, that is, when they have aspect ratios greater than 10.[16] There have been very few reports of optical trapping of metallic nanowires, and these have been limited to Ag nanowires. The first reported attempt to trap Ag nanowires was from Pauzauskie and co-workers;[17] they succeeded in trapping semiconductor nanowires using a focused laser beam, but found Ag nanowires could not be trapped in bulk solution. This result has been verified by other studies,[18,19] which found that single-beam optical traps could confine individual Ag nanowires only in two dimensions next to the surfaces of coverslips. The difficulties stem from the fact that the force associated with radiation pressure on these particles can easily exceed the gradient force responsible for trapping.[11,20,21] In particular,

* Address correspondence to nfschere@uchicago.edu.

Received for review June 24, 2013 and accepted September 16, 2013.

Published online September 16, 2013
10.1021/nn403936z

for Ag nanowires, multiple longitudinal plasmon resonances exist that increase the absorption and scattering cross sections at specific wavelengths and, thus, increase the radiation pressure.[19,22] Consequently, radiation pressure can overwhelm the attractive gradient force, pushing the nanowires out of the optical trap in the beam propagation direction. One approach to obtaining axial optical trapping stability might involve compensating the radiation pressure using two counter-propagating beams.[23] However, since the gradient force was also found to depend on the area of the trapping field that interacts with the nano-objects, Ag nanowires could be trapped in spatially extended beams but not in tightly focused ones.[11,19] As a result, optical trapping of Ag nanowires has been achieved only by using counter-propagating Bessel beams with extended optical fields.[24] For these reasons, it has been widely considered that relatively large metal particles cannot be trapped in three dimensions by (tightly focused) single-beam optical tweezers due to their strong absorption and scattering of light.[11,12,25]

However, this particle-size-based conventional wisdom of what can or cannot be trapped may be oversimplified. Here we present experimental observations showing that a single, tightly focused laser beam with a wavelength of 800 nm can be used for 3D trapping of Au nanowires that are more than 2 μm in length and have aspect ratios greater than 50. The trapped Au nanowires tend to align perpendicular to the light polarization direction, unlike Au nanorods, which align parallel to the polarization.[13,14,26] We have elucidated the reasons for the optical trapping behaviors of Au nanowires using electrodynamics simulations. Detailed comparisons are made to the case of Ag nanowires. As a result, we now understand that the plasmonic properties of metal nanostructures rather than their sizes determine what can or cannot be trapped by single focused Gaussian beams.

RESULTS AND DISCUSSION

Au nanowires with lengths of 1−3 μm and diameters of ~40 nm were used in the experiments. An aqueous solution of the nanowires was contained in a chamber formed by a spacer between two coverslips with a separation of 130 μm, as illustrated in Figure 1a. Figure 1b shows a scanning electron microscope (SEM) image of two representative Au nanowires. A Gaussian laser beam with a wavelength of 800 nm was tightly focused into the chamber. The laser beam propagated in the *z*-direction with the focal plane located at a height, *h*, above the bottom coverslip. The sequential frames, 1−9 of Figure 1c, show the optical trapping of an Au nanowire in bulk solution. We found that, although the nanowires could be trapped by one beam at one end in solution, their orientations were not stable. Frame 10 is a composite image of the trapped nanowires in a period of 3 s. It shows that one

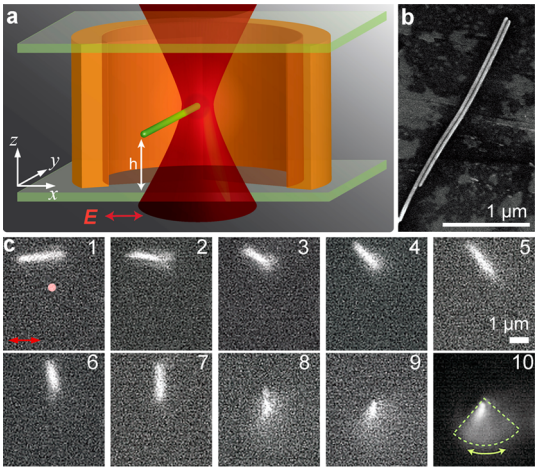

Figure 1. (a) Illustration of an Au nanowire trapped by a single, tightly focused Gaussian laser beam in bulk solution. (b) SEM image of Au nanowires used in the experiments. (c) Experimental demonstration of three-dimensional (3D) optical trapping (see Supporting Information, Movie S1) measured by dark-field microscopy. The focal spot of the laser beam was at $h = 50$ μm as indicated by the red spot, and the laser beam entering the objective has a power of 25 mW. Frames 1−9 show an Au nanowire entering the optical trap. The time step for the frames is 35 ms. Image 10 is a superposition of frames taken over a 3 s window (~ 90 frames) after frame 9. The angular fluctuation of the free end creates a fan (demarcated by the dashed sector).

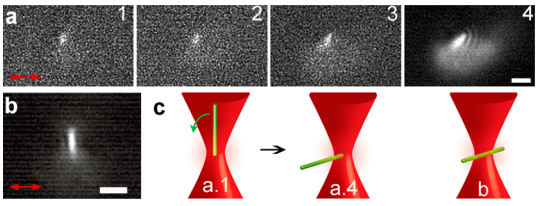

Figure 2. (a) Dark-field images of an Au nanowire trapped by a focused Gaussian beam (see Supporting Information, Movie S2). In frames 1 and 2, the nanowire aligned along the *z*-axis, while in frame 3, it rotated into the *x*−*y* plane. The interval between frames 1 and 2 is 0.72 s, and that between 2 and 3 is 0.07 s. Image 4 is a superposition of frames taken over 3 s after frame 3. The laser power entering the objective is 50 mW, and the laser is focused at $h = 17$ μm. The white scale bar represents 1 μm. (b) An Au nanowire trapped at its midpoint by a focused spot. The image is a superposition of frames taken over 3 s. The laser power is 100 mW, and the laser is focused at $h = 17$ μm. The scale bar is 1 μm. (c) Illustrations of several representative configurations of the nanowires in panels a and b.

end of the nanowire was trapped but the other end underwent angular fluctuations over a range of ~90° in an arc symmetric to the *y*-axis. The radius of the brightened sector is ~2.3 μm, equal to the length of the nanowire, indicating that nanowire was located in the *x*−*y* plane.

Trapped Au nanowires could also align along the beam propagation direction (*z*-direction), as demonstrated in Figure 2a. The particular nanowire shown in Figure 2a1−4 rotated from an axial alignment to being trapped perpendicular to the beam propagation direction, as depicted in Figure 2c.

While the Au nanowires were usually trapped near their ends, we found that trapping at their midpoints was also possible, especially for short nanowires (~1 μm long) and greater laser power (100 mW), as shown in Figure 2b. In this configuration, the nanowire orientations were relatively stable and remained almost perpendicular to the light polarization direction. Multiple nanowires trapped by a single focused beam have been also observed, as shown in Figure S1, Supporting Information.

Typical trapping times of the Au nanowires by the single-beam optical trap were around 14 s at 25 mW laser power (Supporting Information, Figure S2), but trapping longer than 50 s was also observed (see Supporting Information, Movie S3). We found that, when the laser power was increased, the trapping time decreased; for example, a laser power of 100 mW resulted in a trapping time of only ~3 s. This is in contrast to the expectation that higher laser power should lead to a deeper potential well for optical trapping, and should thus increase the trapping stability.[20] Thermal effects may be responsible for the reduced trapping stability at high laser powers, since it is well-known that laser illumination can induce significant heating of Au nanostructures.[27,28] We did not observe bubble formation on the trapped Au nanowires, but the heating at high laser power may reduce the colloidal stability of the nanowires by causing the capping molecules (cetrimonium bromide) to come off their surfaces. Heat dissipation from the nanowires to the surrounding fluid can also result in thermophoretic forces that tend to push the Au nanowires away from the trap.[29] On the other hand, the thermal effect at a laser power of 25 mW is at least not strong enough to lead to nanowire deformation: as shown in Supporting Information, Movie S3 and Figure S3. Even after being trapped for >50 s, the escaping nanowire had maintained its morphology.

We performed 3D finite-difference time-domain (FDTD) simulations to understand the various optical forces that act on the Au nanowires and why these forces lead to stable 3D optical trapping. To reveal why the angular fluctuations shown in Figures 1c and 2a occur, we assumed that one end of an Au nanowire was trapped at the waist of the Gaussian beam and the other end could rotate about the trapped end, so that the nanowire can be oriented at any angle θ relative to the polarization direction. The calculated intensity distributions of the electric field around the nanowire are shown in Figure 3a for different θ. The local electric fields around the nanowire are asymmetric with respect to the long axis for all angles except $\theta = 0°$ and $\theta = 90°$; however, the field distributions are the same for angles below $\theta = 90°$ as they are for angles above $\theta = 90°$. Optical forces on the nanowire can be calculated by integrating the Maxwell stress tensor over a surface surrounding the nanowire, and the results are plotted in Figure 3b. The force along the short axis, F_s, has a maximum absolute value at 45° and 135°, and always exerts a torque to rotate the nanowire toward $\theta = 90°$ (except at the unstable equilibrium point $\theta = 0°$). This is consistent with our observation that the nanowire orientation fluctuates over the angular range of about 45−135°. The force calculation also suggests an electrodynamic factor that affects the trapping stability of Au nanowires. Although, for θ between 45° and 135°, the short-axis force F_s can rotate the nanowire to 90°, the long-axis force F_l becomes negative for $\theta < 60°$ and >120°, as shown in Figure 3b. This means the nanowire tends to be pushed out of the trap when it rotates into the angular ranges of 45−60° and 120−135°. If the nanowire cannot rotate back to 60−120° before it moves out of the trap, the trapping event will end.

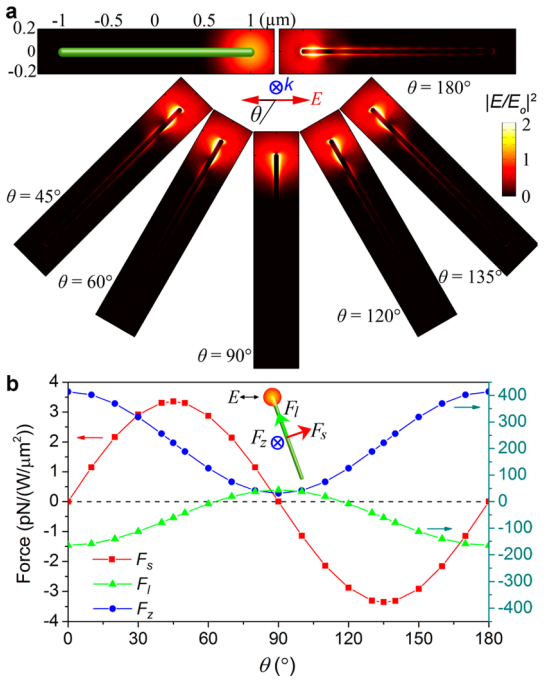

Figure 3. 3D finite-difference time-domain (FDTD) simulations of an Au nanowire illuminated by a linearly polarized Gaussian beam. (a) The top left image shows the model: the nanowire is approximated as an Au cylinder (diameter of 40 nm and length of 2 μm) with hemispherical ends immersed in water and aligned in the $x-y$ plane. The incident Gaussian beam has a wavelength of 800 nm, is linearly polarized along the x-axis, and propagates in the z-direction. One end of the nanowire is located at the waist of the Gaussian beam and the other end is movable. The angle between the long axis of the nanowire and the negative x-direction is denoted as θ. Results are shown for the time-averaged intensity distribution of the electric field, $|E/E_o|^2$, around the nanowire, normalized by the incident intensity. (b) Calculated optical forces on the Au nanowire along its long axis (F_l) and short axis (F_s; note that the nanowire rotates in the $x-y$ plane and F_s is not always in the x-direction), and along the beam propagation direction (F_z) as a function of θ. The positive direction of F_l points toward the center of the Gaussian beam and that of F_s points in the counterclockwise direction.

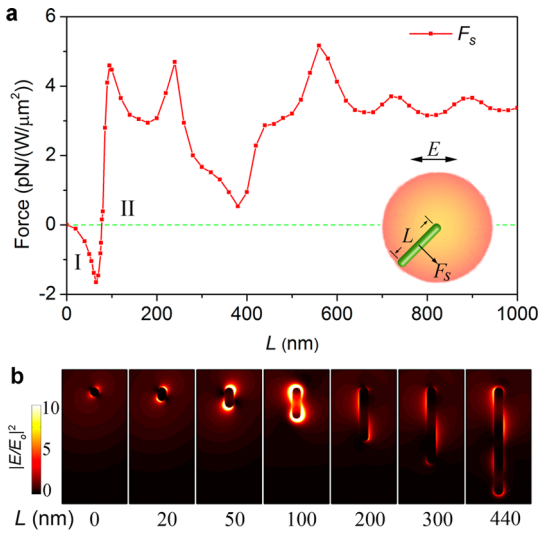

Figure 4. FDTD simulations of Au nanorods and nanowires with diameters of 40 nm, illuminated by a Gaussian beam. (a) The short-axis optical force as a function of the rod/wire length, for θ = 45°. The simulation model is shown in the inset. Note that L is the length of the cylinder while the length of the rod/wire is L plus its diameter, due to the two hemispherical ends. (b) Normalized and time-averaged intensities of the electric field intensity around the Au nanorods/wires.

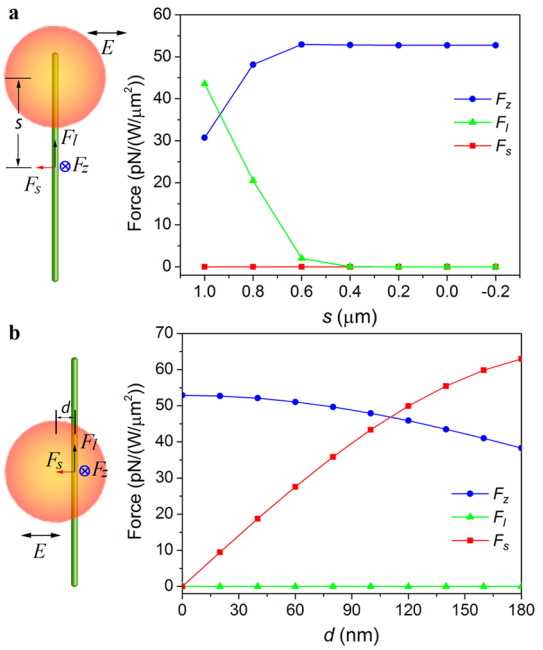

Figure 5. 3D FDTD simulations of an Au nanowire with a length of 2 μm and a diameter of 40 nm, illuminated at different positions by a focused Gaussian beam. (a) The left panel shows the simulation model and the coordinate system: the center of the beam is on the long axis of the nanowire (d = 0), and moves from one end of the nanowire to its midpoint. The right panel shows the calculated optical forces. (b) The center of the beam is now on the short axis crossing the midpoint of the nanowire (s = 0), and the beam moves away along the short axis. The right panel shows the calculated optical forces.

The trends of the angular dependence of the forces are similar for Au nanowires with micrometer lengths (see Supporting Information, Figure S4). However, as the length of the Au nanowire decreases to around 100 nm and becomes a nanorod, the preferred orientation changes. Figure 4a shows the wire length dependence of the short-axis optical force (F_s) on an Au nanowire oriented at 45° to the polarization of the incident beam. Two different regimes can be identified. In regime I, for L < 78 nm, F_s < 0, which means that the nanorods will be rotated toward θ = 0° rather than θ = 90°, consistent with previous experimental studies.[11,12,26] In regime II, for L > 78 nm, F_s > 0, and the nanorods or nanowire is rotated toward θ = 90°, consistent with the current experimental results. The value L = 78 nm, corresponding to a total particle length of 118 nm and an aspect ratio of 3, can thus be considered as the critical length defining the boundary between nanorods and nanowires, at least in the context of optical trapping. For nanorods (regime I), the field enhancement is greatest along the polarization direction, whereas for nanowires (regime II), the field enhancement near the trapped end is greatest perpendicular to the polarization direction. The degree to which longitudinal or transverse modes in a nanowire are excited depends on the wavelength of incident light, so the critical length that defines the boundary between nanorods and nanowires will be somewhat wavelength dependent. When the light polarization is neither parallel nor perpendicular to an Au nanowire, both transverse and longitudinal plasmon resonances are excited in the nanowire. These modes are calculated separately and shown in Figure S5, Supporting Information. Their coherent superposition, as excited by the incident beam, leads to the asymmetric local fields. It is worth noting that, when L is larger than ~440 nm, multiple longitudinal plasmon resonances are supported by the nanowire, resulting in the oscillation of the force curve shown in Figure 4a.[22,30] The oscillation vanishes for L > 2.5 μm (see Supporting Information, Figure S4b, and also Figure 6) due to strong damping of the longitudinal plasmon resonances in Au nanowires.[31]

3D optical trapping requires that all forces acting on the nanowire are balanced at the trapping position. For θ = 90°, the forces F_s and F_l become zero when the nanowire is trapped at its midpoint (Figure 5a). This position and orientation thus represents the most stable configuration in the x–y plane. However, the long axis force (F_l) drops quickly when the trapping position moves from one end of the nanowire to the midpoint, as shown in Figure 5a; this explains why the Au nanowires can still be trapped near their ends.

Moreover, to make 3D optical trapping possible, the gradient force should be as large as the scattering force. In the current simulation, F_z represents a pure scattering force, because the nanowire is located at the center of the beam waist. In the experiments, a trapped particle is located at a position beyond the focal plane

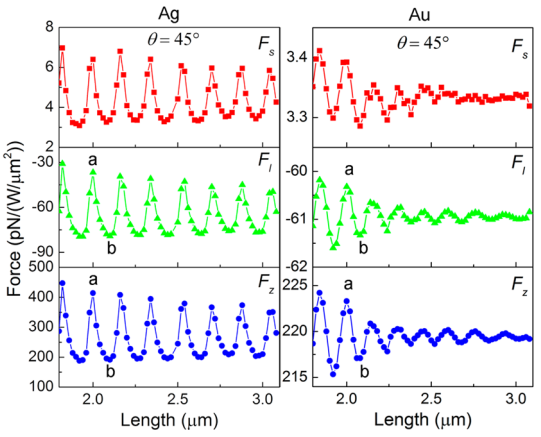

Figure 6. Calculated optical forces exerted by a Gaussian beam on Ag and Au nanowires with lengths of 2 μm and diameters of 40 nm. The configuration is the same as that in Figure 3. Note the change in scale.

along the beam propagation direction (above the focal spot in our experimental geometry).[32,33] However, in our FDTD calculations it is difficult to simulate a Gaussian beam that is tightly focused along its propagation direction. We therefore chose to calculate the gradient force by shifting the nanowire in the transverse direction; in this case, the gradient force is F_s and the force due to radiation pressure is F_z.[20] As shown in Figure 5b, when the Au nanowire was moved away from the center of the beam by a distance d, the gradient force could overcome the radiation pressure for $d > 110$ nm. This indicates that the gradient force in the beam propagation direction can also be strong enough to enable 3D trapping of Au nanowires. Although gravity may play a role in compensating radiation pressure for larger particles,[34] the gravitational force on an Au nanowire with diameter of 40 nm and length of 2 μm is 0.5 fN, much less than the calculated scattering force of at least 4 pN for a laser power of 25 mW.

It is important to understand why single-beam 3D optical trapping is possible for Au nanowires but not Ag nanowires. In our previous study,[19] we used a polydisperse sample of Ag nanowires that also contained nanowires with diameters around 40 nm and lengths of 1−3 μm, but never observed a 3D optical trapping event when using a focused Gaussian beam. Several factors may contribute to the different behaviors. First, the Ag and Au nanowires that we have studied have different surface coatings that will affect their colloidal stability, especially when considering heating in the optical trap. Second, multiple longitudinal plasmon resonances in Ag nanowires lead to increased optical scattering, and thus reduced trapping stability. Figure 6 shows that an Ag nanowire has much stronger multiple longitudinal modes compared to an Au nanowire with the same size, since the plasmon resonances are more strongly damped in Au than in Ag. For a trapped Ag nanowire, the multiple longitudinal modes will cause large variation of the scattering

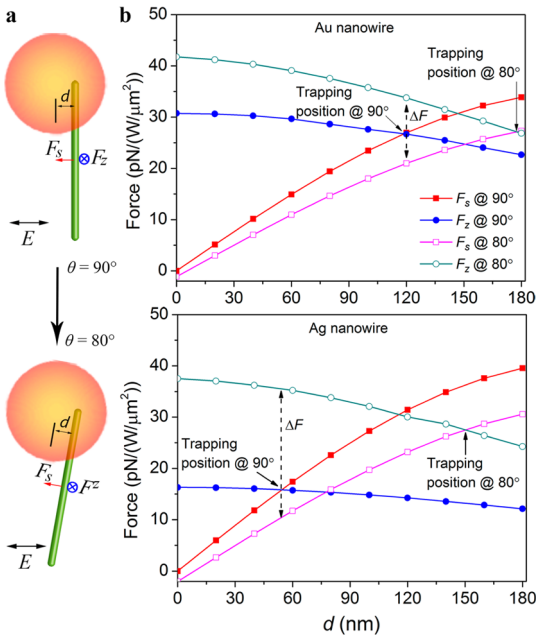

Figure 7. Calculated gradient and scattering forces exerted by a Gaussian beam on Ag and Au nanowires with lengths of 2 μm and diameters of 40 nm. (a) Illustration of the simulation model: the nanowire is trapped at one end at a distance d from the beam center. Two orientations are modeled: θ = 90° and θ = 80°. (b) Calculated forces as a function of d.

force on the nanowire as it undergoes angular fluctuations. We suspect that these fluctuations may make the Ag nanowire unstable in a tightly focused Gaussian optical trap. Since the longitudinal plasmon resonances occur at specific wavelengths that depend on the length of the nanowire, the absorption and scattering cross sections, and therefore the optical forces, will depend on wavelength.[19] This variation means that, at a given wavelength (such as 800 nm used in the current experiments), nanowires with certain lengths are favorable for optical trapping while those with different lengths are not. However, for a polydisperse sample with different lengths of nanowires, there will be some nanowires whose lengths should be favorable for trapping. The fact that 3D optical trapping of Ag nanowires was never observed before suggests that Ag nanowires are not trappable by single-beam optical tweezers.

In Figure 7, we calculated the gradient and scattering forces on Ag and Au nanowires with the same size. We began by assuming the nanowires were trapped at their ends with $\theta = 90°$ (*i.e.*, the stable orientation). The results indicate that the gradient force exceeds the radiation pressure for both Au and Ag nanowires, so that in principle they can both be trapped in this orientation. We then assumed the nanowires undergo a certain degree of angular fluctuations, as observed in the experiments. As an example, we calculated the forces when the nanowires rotated to $\theta = 80°$. The results show that, for both Au and Ag nanowires, the gradient force decreases and the radiation pressure

increases due to the excitation of longitudinal plasmon resonances. This will induce a gap, ΔF, between the two forces, which destabilizes the trapping and pushes the nanowire further from the center of the focus. The force gap is 13 pN/(W/μm^2) for the Au nanowire, and 26 pN/(W/μm^2) for the Ag nanowire, which means that the Au nanowire needs to move a distance Δd = 58 nm until it reaches the trapping position, whereas the Ag nanowire needs to move Δd = 97 nm. During this process, the trapping is not stable, so that the Ag nanowire will be more likely to escape. We believe that this sensitivity to angular fluctuations is an important reason why single-beam optical tweezers cannot trap Ag nanowires in three dimensions but can trap Au nanowires.

CONCLUSIONS

We have demonstrated that single Au nanowires can be trapped in three dimensions by single-beam optical traps. The experimental findings are corroborated by electrodynamics simulations. These results extend the list of plasmonic nanostructures that can be trapped in three dimensions by single-beam optical tweezers from nanoparticles and nanorods to much longer nanowires, which were formerly considered impossible to trap.[12,21] The results indicate that the previous concern—that absorption and scattering in large metal particles are too strong to allow single-beam optical trapping—is overly simplified. Other issues, such as colloidal stability and thermal effects, may play a role in determining which particles can and cannot be trapped, as well as the fact that absorption and scattering depend strongly on the composition and geometry of the metal particles. Our findings indicate that it will be possible to stably trap and manipulate Au nanowires in three dimensions using multiple-spot holographic optical tweezers,[35] enabling fabrication of functional nanoplasmonic systems.

The ability to optically control and manipulate Au nanowires in three dimensions will benefit both fundamental investigations and applications. For example, when studying the acoustic vibrations of single nanostructures, it is desirable to keep the nanostructures away from substrates to avoid mechanical coupling.[36,37] For Au nanowires, this could be partially achieved by suspending them over a trench fabricated in a substrate.[36] In contrast, 3D optical trapping would provide a truly homogeneous environment for the nanowires.[37] Optically trapped Au nanowires may also serve as probes for biological detection. For example, cytokine-carrying Au nanowires have been manipulated by electric fields to stimulate prespecified cells and reveal signaling events.[38] Optical trapping represents an alternative approach,[9] and our results provide the understanding required to take advantage in these applications of the large, plasmon-induced, near-field optical enhancement next to the nanowires.

METHODS

The experiments were conducted with an optical tweezers system that we have previously described in detail.[24] A single Gaussian beam from a cw-Ti:Sapphire laser (wavelength = 800 nm) was focused by a 60× water immersion objective (NA 1.2, Olympus UPLSAPO). The 800 nm wavelength is far to the red side of the transverse plasmon resonance of Au nanowires (approximately 520−550 nm), so laser-induced thermal effects could be minimized. The Au nanowires were synthesized using a seeded growth process with Au nanorods as the seeds.[39] The nanowires were approximately 1−3 μm in length and ~40 nm in diameter and were stabilized by cetrimonium bromide. These Au nanowires underwent Brownian motion in the sample cell, and slowly settled to the bottom coverslip on time scales longer than the duration of a single experiment. (An experiment was usually done within 20 min). The nanowires were imaged by dark-field microcopy. The laser light scattered from the nanowires was blocked by a short-pass filter (cutoff edge at 650 nm). A Firewire camera (Sony XCD-V60) was used to record the images.

The commercial software package "FDTD Solutions" (Lumerical, Inc.) was used for electrodynamics simulations. In the models, a nanowire is approximated as a cylinder with hemispherical ends. The nanowire is illuminated by a linearly polarized Gaussian beam with a waist diameter of 700 nm and (vacuum) wavelength of 800 nm. The refractive index of Au is set as $n = 0.15 + i4.91$ and that of Ag is set as $n = 0.04 + i5.57$.[40] The nanowire is immersed in water (n = 1.33). A nonuniform mesh with maximum grid size of 4 nm is used. The optical forces on the nanowire are calculated by integrating the Maxwell stress tensor (T_{ij}) over a surface (s) surrounding the nanowire:[20]

$$\langle F_i \rangle = \frac{1}{2} \mathrm{Re}\left(\int_s T_{ij} n_j ds \right) \quad (1)$$

where $\langle \cdots \rangle$ indicates a time averaged value, Re indicates the real part of a complex number, and n_j are the vector components of the normal pointing outward from the surface. The optical forces are generally decomposed into the gradient force F_{grad}, the scattering force F_{scat}, and the absorption force F_{abs}:[20]

$$F_{grad} = \frac{1}{2} \mathrm{Re}(\alpha) \nabla \langle E^2 \rangle \quad (2)$$

$$F_{abs} = \frac{n_m}{c} \langle P \rangle C_{abs} \quad (3)$$

$$F_{scat} = \frac{n_m}{c} \langle P \rangle C_{scat} \quad (4)$$

where α is the Au nanowire's complex polarizability, E is the electric field, n_m is the refractive index of the host medium, c is the speed of light, P is the Poynting vector, and C_{abs} and C_{scat} are the absorption and scattering cross sections, respectively. The results of the calculated optical forces are shown in Figures 3−7.

Conflict of Interest: The authors declare no competing financial interest.

Acknowledgment. We acknowledge support from the U.S. Department of Energy (DOE), Office of Science, Division of Chemical, Geological and Biological Sciences under Contract No. DE-AC02-06CH11357, and the NSF (CHE-1059057). This work was performed, in part, at the Center for Nanoscale Materials, a U.S. Department of Energy, Office of Science, Office of Basic Energy Sciences User Facility under Contract No. DE-AC02-06CH11357. E.R.Z. acknowledges financial support from the National Science Foundation (DMR-1105878).

Supporting Information Available: Video clips showing the optical trapping of Au nanowires and additional figures.

This material is available free of charge *via* the Internet at http://pubs.acs.org.

REFERENCES AND NOTES

1. Pelton, M.; Bryant, G. *Introduction to Metal-Nanoparticle Plasmonics*; John Wiley & Sons: Hoboken, NJ, 2013.
2. Xia, Y. N.; Halas, N. J. Shape-Controlled Synthesis and Surface Plasmonic Properties of Metallic Nanostructures. *MRS Bull.* **2005**, *30*, 338–344.
3. Jain, P. K.; Huang, X.; El-Sayed, I. H.; El-Sayed, M. A. Noble Metals on the Nanoscale: Optical and Photothermal Properties and Some Applications in Imaging, Sensing, Biology, and Medicine. *Acc. Chem. Res.* **2008**, *41*, 1578–1586.
4. Ohlinger, A.; Nedev, S.; Lutich, A. A.; Feldmann, J. Optothermal Escape of Plasmonically Coupled Silver Nanoparticles from a Three-Dimensional Optical Trap. *Nano Lett.* **2011**, *11*, 1770–1774.
5. Ruijgrok, P. V.; Zijlstra, P.; Tchebotareva, A. L.; Orrit, M. Damping of Acoustic Vibrations of Single Gold Nanoparticles Optically Trapped in Water. *Nano Lett.* **2012**, *12*, 1063–1069.
6. Nome, R. A.; Guffey, M. J.; Scherer, N. F.; Gray, S. K. Plasmonic Interactions and Optical Forces between Au Bipyramidal Nanoparticle Dimers. *J. Phys. Chem. A* **2009**, *113*, 4408–4415.
7. Dienerowitz, M.; Mazilu, M.; Reece, P. J.; Krauss, T. F.; Dholakia, K. Optical Vortex Trap for Resonant Confinement of Metal Nanoparticles. *Opt. Express* **2008**, *16*, 4991–4999.
8. Prikulis, J.; Svedberg, F.; Käll, M.; Enger, J.; Ramser, K.; Goksor, M.; Hanstorp, D. Optical Spectroscopy of Single Trapped Metal Nanoparticles in Solution. *Nano Lett.* **2004**, *4*, 115–118.
9. Nakayama, Y.; Pauzauskie, P. J.; Radenovic, A.; Onorato, R. M.; Saykally, R. J.; Liphardt, J.; Yang, P. Tunable Nanowire Nonlinear Optical Probe. *Nature* **2007**, *447*, 1098.
10. Bosanac, L.; Aabo, T.; Bendix, P. M.; Oddershede, L. B. Efficient Optical Trapping and Visualization of Silver Nanoparticles. *Nano Lett.* **2008**, *8*, 1486–1491.
11. Svoboda, K.; Block, S. M. Optical Trapping of Metallic Rayleigh Particles. *Opt. Lett.* **1994**, *19*, 930–932.
12. Hansen, P. M.; Bhatia, V. K.; Harrit, N.; Oddershede, L. Expanding the Optical Trapping Range of Gold Nanoparticles. *Nano Lett.* **2005**, *5*, 1937–1942.
13. Pelton, M.; Liu, M. Z.; Kim, H. Y.; Smith, G.; Guyot-Sionnest, P.; Scherer, N. E. Optical Trapping and Alignment of Single Gold Nanorods by Using Plasmon Resonances. *Opt. Lett.* **2006**, *31*, 2075–2077.
14. Selhuber-Unkel, C.; Zins, I.; Schubert, O.; Soennichsen, C.; Oddershede, L. B. Quantitative Optical Trapping of Single Gold Nanorods. *Nano Lett.* **2008**, *8*, 2998–3003.
15. Toussaint, K. C., Jr.; Liu, M.; Pelton, M.; Pesic, J.; Guffey, M. J.; Guyot-Sionnest, P.; Scherer, N. F. Plasmon Resonance-Based Optical Trapping of Single and Multiple Au Nanoparticles. *Opt. Express* **2007**, *15*, 12017–12029.
16. Chen, J.; Wiley, B. J.; Xia, Y. One-Dimensional Nanostructures of Metals: Large-Scale Synthesis and Some Potential Applications. *Langmuir* **2007**, *23*, 4120–4129.
17. Pauzauskie, P. J.; Radenovic, A.; Trepagnier, E.; Shroff, H.; Yang, P. D.; Liphardt, J. Optical Trapping and Integration of Semiconductor Nanowire Assemblies in Water. *Nat. Mater.* **2006**, *5*, 97–101.
18. Tong, L.; Miljkovic, V. D.; Käll, M. Alignment, Rotation, and Spinning of Single Plasmonic Nanoparticles and Nanowires Using Polarization Dependent Optical Forces. *Nano Lett.* **2010**, *10*, 268–273.
19. Yan, Z.; Sweet, J.; Jureller, J. E.; Guffey, M. J.; Pelton, M.; Scherer, N. F. Controlling the Position and Orientation of Single Silver Nanowires on a Surface Using Structured Optical Fields. *ACS Nano* **2012**, *6*, 8144–8155.
20. Dienerowitz, M.; Mazilu, M.; Dholakia, K. Optical Manipulation of Nanoparticles: A Review. *J. Nanophotonics* **2008**, *2*, 021875.
21. Sato, S.; Harada, Y.; Waseda, Y. Optical Trapping of Microscopic Metal Particles. *Opt. Lett.* **1994**, *19*, 1807–1809.
22. Ditlbacher, H.; Hohenau, A.; Wagner, D.; Kreibig, U.; Rogers, M.; Hofer, F.; Aussenegg, F. R.; Krenn, J. R. Silver Nanowires as Surface Plasmon Resonators. *Phys. Rev. Lett.* **2005**, *95*, 257403.
23. Zemanek, P.; Jonas, A.; Sramek, L.; Liska, M. Optical Trapping of Nanoparticles and Microparticles by a Gaussian Standing Wave. *Opt. Lett.* **1999**, *24*, 1448–1450.
24. Yan, Z.; Jureller, J. E.; Sweet, J.; Guffey, M. J.; Pelton, M.; Scherer, N. F. Three-Dimensional Optical Trapping and Manipulation of Single Silver Nanowires. *Nano Lett.* **2012**, *12*, 5155–5161.
25. Lehmuskero, A.; Ogier, R.; Gschneidtner, T.; Johansson, P.; Käll, M. Ultrafast Spinning of Gold Nanoparticles in Water Using Circularly Polarized Light. *Nano Lett.* **2013**, *13*, 3129–3134.
26. Ruijgrok, P. V.; Verhart, N. R.; Zijlstra, P.; Tchebotareva, A. L.; Orrit, M. Brownian Fluctuations and Heating of an Optically Aligned Gold Nanorod. *Phys. Rev. Lett.* **2011**, *107*, 037401.
27. Guffey, M. J.; Scherer, N. F. All-Optical Patterning of Au Nanoparticles on Surfaces Using Optical Traps. *Nano Lett.* **2010**, *10*, 4302–4308.
28. Baffou, G.; Quidant, R.; García de Abajo, F. J. Nanoscale Control of Optical Heating in Complex Plasmonic Systems. *ACS Nano* **2010**, *4*, 709–716.
29. Garces-Chavez, V.; Quidant, R.; Reece, P. J.; Badenes, G.; Torner, L.; Dholakia, K. Extended Organization of Colloidal Microparticles by Surface Plasmon Polariton Excitation. *Phys. Rev. B* **2006**, *73*, 085417.
30. Cao, L.; Nome, R. A.; Montgomery, J. M.; Gray, S. K.; Scherer, N. F. Controlling Plasmonic Wave Packets in Silver Nanowires. *Nano Lett.* **2010**, *10*, 3389–3394.
31. Wild, B.; Cao, L.; Sun, Y.; Khanal, B. P.; Zubarev, E. R.; Gray, S. K.; Scherer, N. F.; Pelton, M. Propagation Lengths and Group Velocities of Plasmons in Chemically Synthesized Gold and Silver Nanowires. *ACS Nano* **2012**, *6*, 472–482.
32. Kyrsting, A.; Bendix, P. M.; Oddershede, L. B. Mapping 3D Focal Intensity Exposes the Stable Trapping Positions of Single Nanoparticles. *Nano Lett.* **2013**, *13*, 31–35.
33. Wang, F.; Toe, W. J.; Lee, W. M.; McGloin, D.; Gao, Q.; Tan, H. H.; Jagadish, C.; Reece, P. J. Resolving Stable Axial Trapping Points of Nanowires in an Optical Tweezers Using Photoluminescence Mapping. *Nano Lett.* **2013**, *13*, 1185–1191.
34. O'Neil, A. T.; Padgett, M. J. Three-Dimensional Optical Confinement of Micron-Sized Metal Particles and the Decoupling of the Spin and Orbital Angular Momentum within an Optical Spanner. *Opt. Commun.* **2000**, *185*, 139–143.
35. Agarwal, R.; Ladavac, K.; Roichman, Y.; Yu, G. H.; Lieber, C. M.; Grier, D. G. Manipulation and Assembly of Nanowires with Holographic Optical Traps. *Opt. Express* **2005**, *13*, 8906–8912.
36. Major, T. A.; Crut, A.; Gao, B.; Lo, S. S.; Del Fatti, N.; Vallée, F.; Hartland, G. V. Damping of the Acoustic Vibrations of a Suspended Gold Nanowire in Air and Water Environments. *Phys. Chem. Chem. Phys.* **2013**, *15*, 4169–4176.
37. Marty, R.; Arbouet, A.; Girard, C.; Mlayah, A.; Paillard, V.; Lin, V. K.; Teo, S. L.; Tripathy, S. Damping of the Acoustic Vibrations of Individual Gold Nanoparticles. *Nano Lett.* **2011**, *11*, 3301–3306.
38. Fan, D. L.; Yin, Z. Z.; Cheong, R.; Zhu, F. Q.; Cammarata, R. C.; Chien, C. L.; Levchenko, A. Subcellular-Resolution Delivery of a Cytokine through Precisely Manipulated Nanowires. *Nat. Nanotechnol.* **2010**, *5*, 545–551.
39. Critchley, K.; Khanal, B. P.; Górzny, M. Ł.; Vigderman, L.; Evans, S. D.; Zubarev, E. R.; Kotov, N. A. Near-Bulk Conductivity of Gold Nanowires as Nanoscale Interconnects and the Role of Atomically Smooth Interface. *Adv. Mater.* **2010**, *22*, 2338–2342.
40. Johnson, P. B.; Christy, R. W. Optical Constants of the Noble Metals. *Phys. Rev. B* **1972**, *6*, 4370–4379.